4th URSI AT-RASC, Gran Canaria, 19-24 May 2024

A Highly-stacked Quantum-dot Mode-locked Laser Comb with 106-GHz Mode Spacing Enabling 4.48-Tb/s IM-DD Transmission Capacity

Paikun Zhu*(1), Yuki Yoshida(1), Atsushi Matsumoto(1), Yuya Yamaguchi(1), Zu-Kai Weng(1), Naokatsu Yamamoto(1), Ken-ichi Kitayama(1)(2), and Kouichi Akahane(1)
(1) National Institute of Information and Communications Technology (NICT), Koganei, Japan *pkzhu3@nict.go.jp
(2) Hamamatsu Photonics Central Research Laboratory, Hamamatsu, Japan

Abstract

We design and fabricate a 15-layer highly-stacked quantum-dot mode-locked laser comb operating in C-band with 106GHz mode spacing. A 4.48-Tb/s (56λ×80Gb/s) aggregated IM-DD transmission capacity is experimentally demonstrated, meeting the BER threshold of standard 7% hard-decision FEC. To the best of our knowledge, this device enables the highest aggregated capacity among QD-MLL-based IM-DD systems.

1. Introduction

Future intra-datacenter networks and other short-reach networks call for high-speed and cost-effective fiber-optic transmission systems, e.g., based on intensity modulation and direct detection (IM-DD). Wavelength division multiplexing (WDM) is a key technique for capacity enhancement without the need to deploy extra fibers. In addition to transmission in O-band which is currently under active discussion, C-band can readily support denser WDM with mature component technology and less impact from fiber nonlinearity; thus, the C-band WDM systems are still worth investigating.

These short-reach WDM systems require efficient and compact multi-wavelength light sources, e.g., optical frequency combs. Mode-locked laser (MLL) is one of the promising options for a low-cost and small-footprint (integrable) comb source. Compared with traditional MLLs based on multi-quantum-well gain medium structure, recently lower-dimensional quantum-dot (QD) or quantum dash (QDash) based MLL devices operating at C-band [1-4] and O-band [5-9] have caught great interest as they have potential benefits of lower threshold current, faster carrier dynamics and also better temperature stability. For future WDM systems, higher channel spacing is preferred, aligning with the trend of higher bit-rate or baud-rate per wavelength [10]. This corresponds to a larger (Fabry-Perot) comb spacing or repetition rate, which means that the MLL devices should have a shorter cavity. However, a short cavity limits the achievable MLL gain and power [7]. To simultaneously achieve a large comb spacing and a large amount of comb lines/tones (each with sufficient tone-to-noise ratio as a signal carrier), a high volume of QD density is needed to obtain more material gain, and a higher stack of QD layers is desired [11]. However, stacking more than 10 QD layers has been a challenging issue [11], and was rarely explored in prior works.

Recently, we reported an advanced growth technique to achieve a 15-layer highly stacked QD, which enabled a fabricated QD-MLL chip with 81-GHz mode spacing and a high count of comb lines [12]. In this work, we further report a newly-fabricated highly-stacked QD-MLL chip operating in the (super-) C-band with ~106-GHz mode spacing. Based on it, an aggregated capacity of 4.48-Tb/s (56λ×80Gb/s) is experimentally confirmed with IM-DD in optical back-to-back (BTB) condition. The achieved aggregated capacity is significantly higher than the previous record of C-band QD-MLL-based IM-DD transmission (2.24-Tb/s) [3] and is also higher than the O-band state-of-the-art (4.1-Tb/s) [6]. The performance of multiple wavelengths after 600m single-mode fiber (SMF) transmission was tested as well.

2. Device Design and Experimental Results

2.1 Device Structure and Characteristics

Figure 1(a) shows the designed layer structure of the two-section QD-MLL waveguide [12]. The layer structure was grown through solid-source molecular beam epitaxy (MBE) with n-type InP(311)B substrates. A 150nm-thick lattice-matched n-type InAlAs cladding layer and a 50nm-thick undoped InGaAlAs waveguide layer were grown on the cleaned surface. Following this, a 20nm-thick InGaAlAs strain-compensating layer and a 2.9ML InAs QD layer were grown. This process was repeated 15 times to create a highly stacked QD structure. A 50nm-thick undoped InGaAlAs waveguide layer was then grown. Finally, a 1600nm-thick p-type InAlAs upper cladding layer and a p-type InGaAs contact layer were grown. Subsequent fabrication steps included UV lithography, dielectric material layer deposition, dry etching, and metal evaporation. A waveguide structure with a 2μm-wide ridge was formed during this process and embedded using BCB. The upper electrode (p-type side) was partitioned into two sections: a 440μm-long gain region and a 50μm-long saturable absorber (SA) region, with a 10μm gap separating the two parts. The waveguide, cleaved to approximately 382μm-long, had one facet coated with a high-reflection

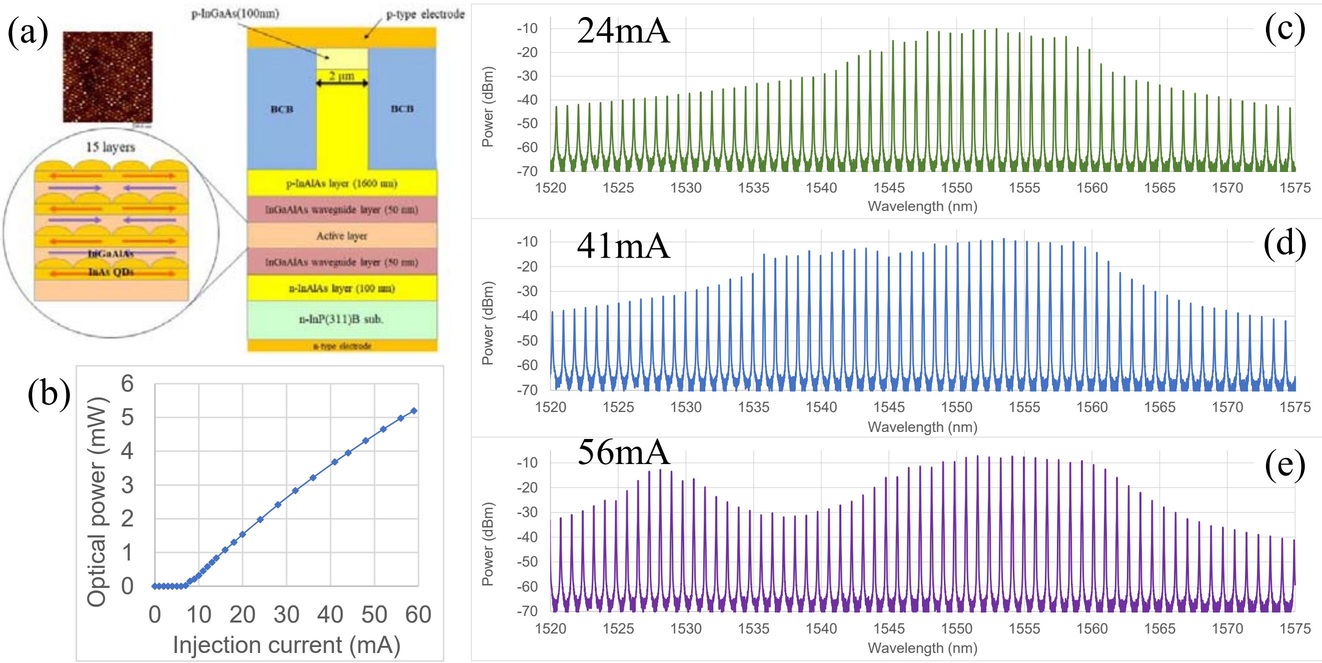

Figure 1. (a) Device structure of the designed QD-MLL. (b) Measured I-L characteristic of the fabricated QD-MLL prototype. (c)-(e) Measured optical spectra of the QD-MLL with injection current at 24mA, 41mA and 56mA.

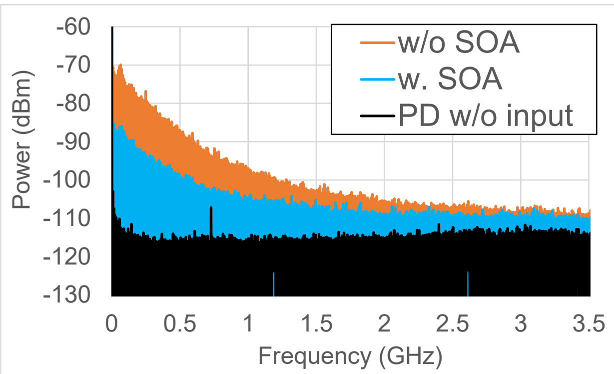

Figure 2. Intensity noise of 1 filtered comb line (at ~1550nm) of the QD-MLL comb. ESA resolution bandwidth: 100Hz.

dielectric mirror. Subsequently, the fabricated chip was mounted to a copper stem, and the two upper electrodes were linked to the external electrode through wire bonding. A direct current (DC) source was employed as the current supplier in the gain region, while a bipolar power supplier served as the bias supplier in the SA region. The light from the as-cleaved side of the chip was captured using an aspherical lens with an antireflection coating, and it was then guided into SMF. The operation temperature was fixed at 20°C.

Figure 1(b) shows the measured relationship between the injection current and output power of the QD-MLL (i.e., I–L characteristics). A bias voltage of +2.0 V within the saturation absorption (SA) region was applied [12]. The maximum positive voltage was determined to prevent damage to the device with sufficient margin. A small threshold current of 7-mA was achieved. The coupling loss from MLL output to the lens can be further optimized toward higher optical power. In addition, Fig. 1(c) shows the optical spectra measured by an optical spectrum analyzer (OSA, Yokogawa AQ6370C) with different injection currents. The mode spacing (or comb line spacing) was approximately 106GHz. In the following experiments, we used an injection current of 41mA corresponding to a MLL power of approximately 5.7dBm.

The intensity noise of the QD-MLL (1 filtered comb line at about 1550nm) was measured using a 42GHz Thorlabs photodetector (PD) and an electrical signal analyzer (ESA, Keysight N9010B). The filtered comb line was amplified by an EDFA from <-10dBm to 12dBm (to mimic the transmission experiment configuration) and then attenuated to prevent PD damage; the PD current was ~0.68mA. Fig. 2(a) shows the frequency-dependent intensity noise; the intensity noise was effectively suppressed using a gain-saturated semiconductor optical amplifier (SOA, operating at 305mA and 23°C with 9dBm input power & 12dBm output power) placed after the EDFA. The optical linewidth of one filtered comb line (~1554nm), measured using the delayed self-heterodyne technique, was about 15-MHz (without SOA) and about 30-MHz (with SOA).

2.2 Data Transmission Performance

Figure 3(a) shows the experimental setup for QD-MLL-driven data transmission. At the transmitter side, the output from the QD-MLL comb passed through 2 stages of optical isolator to prevent damage to the chip. A tunable optical bandpass filter (OBPF) with ~50GHz bandwidth filtered out 1 comb tone (at different wavelengths). After an EDFA, a gain-saturated SOA and a polarization controller (PC), the ~11dBm tone was sent for optical modulation via a Mach-Zehnder modulator (MZM). An 80GBd root raised cosine (RRC) shaped electrical on-off keying (OOK) signal

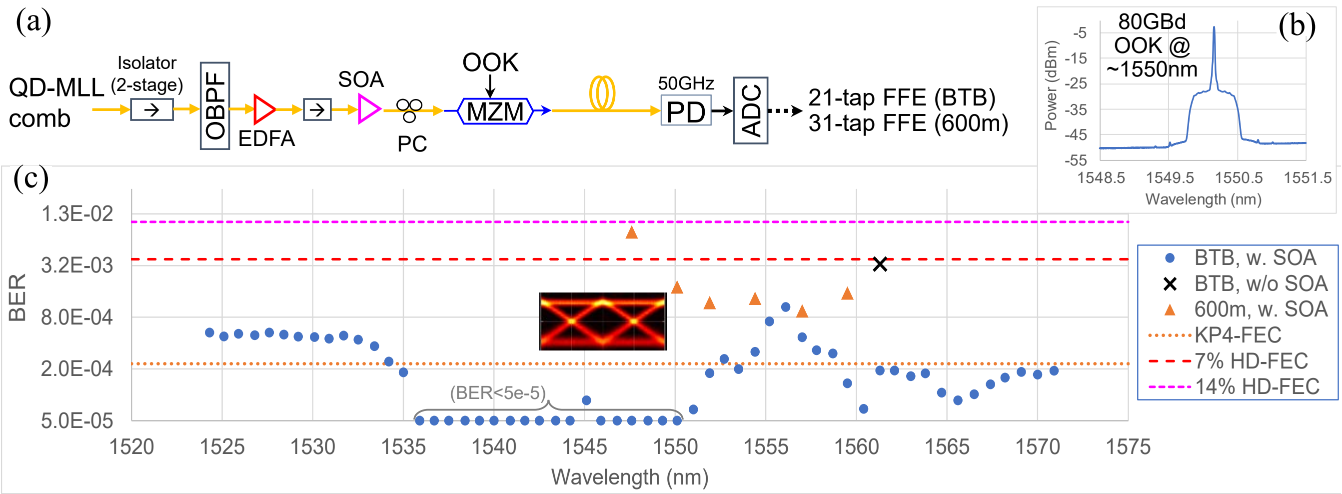

Figure 3. (a) Experimental setup for data transmission. PC: polarization controller. FFE: feedforward equalizer. BTB: back-to-back (with 2m patchcord). (b) Optical spectra of 80GBd OOK signal at ~1550nm. (c) Measured BER results. The inset shows an eye diagram (after equalization) of 80GBd OOK signal (BTB case) at ~1550nm.

was generated by a 256GS/s arbitrary waveform generator (AWG, Keysight M8199A). The roll-off factor of the RRC filter was 0.25 so that the signal bandwidth was confined to 100GHz to fit the WDM comb line spacing of 106GHz. The peak-to-peak voltage (V_{pp}) of the signal was 1.2V. The MZM was biased slightly below the quadrature point and the output power with modulation was about 1dBm. The optical OOK signal was then transmitted in a back-to-back (BTB) condition (with a 2m patchcord) or over 600m SMF to the receiver, which was detected by a 50GHz PD and captured by a 256GSa/s analog-to-digital converter (ADC, Keysight real-time oscilloscope). The receiver did not involve optical or electrical amplifiers. The offline digital signal processing (DSP) includes resampling, matched RRC filtering, downsampling & synchronization, symbol-spaced FFE, and BER calculation by direct error counting (>10^6 bits counted). Fig. 3(b) shows the optical spectra of the QD-MLL-generated 80GBd OOK signal at one wavelength (~1550nm).

Figure 3(c) shows the measured BER versus 80GBd OOK signals at 56 different wavelength channels in BTB case; 21-tap FFE was used. The BER of all measured 56 channels met the 7% hard-decision forward error correction (HD-FEC) limit (BER=3.8e-3) [6, 7]. Besides, BERs of more than 30 channels were better than the KP4 FEC limit (BER=2.4e-4) [13]. The aggregated capacity was 4.48-Tb/s (56λ×80Gb/s) and >4.18-Tb/s excluding 7% FEC overhead. These channels span the super C-band [14]; the capacity in the standard C-band was 3.36-Tb/s (42λ×80Gb/s). Moreover, a 10-fold BER reduction by using a saturated SOA for intensity noise suppression was observed. We also measured the performance of multiple wavelength channels after 600m SMF transmission (with 31-tap FFE); all exhibited BER better than the 14.3% HD-FEC threshold (BER=1.03e-2) [15]. The penalties compared with BTB case could be due to the noise transfer from phase noise to intensity noise.

3. Conclusion

We have designed and fabricated a 15-layer highly-stacked quantum-dot mode-locked laser (QD-MLL) comb operating in (super-) C-band with 106GHz mode spacing and an output power of nearly 6dBm (20°C operating temperature, +2V bias voltage, 41mA injection current). The characterization results show a record 4.48-Tb/s aggregated IM-DD transmission capacity.

References

[1] V. Vujicic, C. Calo, R. Watts, F. Lelarge, C. Browning, K. Merghem, A. Martinez, A. Ramdane, and L. P. Barry, "Quantum Dash Mode-Locked Lasers for Data Centre Applications," IEEE JSTQE, vol. 21, no. 6, p. 1101508, 2015.

[2] N. Eiselt, H. Griesser, M. Eiselt, W. Kaiser, S. Aramideh, J. J. V. Olmos, I. T. Monroy, and J.-P. Elbers, "Real-time 200 Gb/s (4× 56.25 Gb/s) PAM-4 Transmission Over 80 km SSMF Using Quantum-dot Laser and Silicon Ring-modulator," Proc. OFC 2017, paper W4D.3.

[3] Z. Lu, J. Liu, L. Mao, C.-Y. Song, J. Weber, D. Poitras, and P. Poole, "2.24 Tbit/s PAM-4 Transmission by an InAs/InP Quantum Dot Mode-Locked Laser," Proc. SPIE, vol. 10946, paper 109460A-2.

[4] M. Al-Qadi, C. Laperle, D. Charlton, M. O'Sullivan, C. Xie, and R. Hui, "Multichannel 16-QAM Single-Sideband Transmission and Kramers–Kronig Detection Using a Single QD-MLL as the Light Source," J. Lightwave Technol., vol. 38, no. 22, pp. 6163-6169, 2020.

[5] C.-H. Chen, M. A. Seyedi, M. Fiorentino, D. Livshits, A. Gubenko, S. Mikhrin, V. Mikhrin, and R. G. Beausoleil, "A comb laser-driven DWDM silicon photonic transmitter based on microring modulators," Optics Express, vol. 23, no. 16, pp. 21541-21548, 2015.

[6] S. Liu, X. Wu, D. Jung, J. C. Norman, M. J. Kennedy, H. K. Tsang, A. C. Gossard, and J. E. Bowers, "High-channel-count 20 GHz passively mode-locked quantum dot laser directly grown on Si with 4.1 Tbit/s transmission capacity," Optica, vol. 6, no. 2, pp. 128-134, 2019.

[7] S. Pan, H. Zhang, Z. Liu, M. Liao, M. Tang, D. Wu, X. Hu, J. Yan, L. Wang, M. Guo, Z. Wang, T. Wang, P. M. Smowton, A. Seeds, H. Liu, X. Xiao and S.

Chen, "Multi-wavelength 128Gbit s^{-1} λ^{-1} PAM4 optical transmission enabled by a 100 GHz quantum dot mode-locked optical frequency comb," J. Phys. D: Appl. Phys., vol. 55, p. 144001, 2022.

[8] J.-Z. Huang Z.-T. Ji, J.-J. Chen, W.-Q. Wei, J.-L. Qin, Z.-H. Wang, Z.-Y. Li, T. Wang, X. Xiao, and J.-J. Zhang, "Ultra-broadband flat-top quantum dot comb lasers," Photonics Research, vol. 10, no. 5, pp. 1308-1316, 2022.

[9] L. Venkatasubramani, H. Xu, M. Buyalo, A. Gubenko, Y. Yu and L. Barry, "100 Gbps/λ Transmission with Quantum Dot O-Band Comb Source using 50 GBd PAM4/16QAM-OFDM Signals," Proc. OFC 2023, paper M4C.6.

[10] H. Isono, "Latest standardization trend for next-gen high speed optical transceivers," Proc. SPIE OPTO, vol. 12027, pp. 147-152, 2022.

[11] F. Tanoue, H. Sugawara, K. Akahane, and N. Yamamoto, "99-μm-long-cavity Laser Diode Using Highly Stacked InGaAs Quantum Dots," Proc. CLEO 2012, paper CM1I.4.

[12] K. Akahane, A. Matsumoto, T. Umezawa, and N. Yamamoto, "High-frequency Short-Pulse Generation With A Highly Stacked Inas Quantum Dot Mode-locked Laser Diode," Japanese Journal of Applied Physics, vol. 60, paper SBBH02, 2021.

[13] R. Nagarajan, I. Lyubomirsky and O. Agazzi, "Low power DSP-based transceivers for data center optical fiber communications," J. Lightwave Technol., vol. 39, no. 16, pp. 5221-5231, Aug. 2021.

[14] X. Liu, "Enabling optical network technologies for 5G and beyond," J. Lightwave Technol., vol. 40, no. 2, pp. 358-367, 2022.

[15] L. M. Zhang and F. Kschischang, "Staircase codes With 6% to 33% overhead," J. Lightwave Technol., vol. 32, no. 10, pp. 1999-2002, 2014.